Halogen-free Photosensitizers based on *meso*-enamine-BODIPYs for bioimaging and photodynamic therapy

Ruth Prieto-Montero,[1†] Aitor Díaz Andres,[2†]Alejandro Prieto-Castañeda,[3†] Andrea Tabero,[4] Asier Longarte,[5] Antonia R. Agarrabeitia,[3,6] Angeles Villanueva[4], María J. Ortiz,[3] Raúl Montero,[7*] David Casanova[2,8*] and Virginia Martínez-Martínez[1*]

Index

1. Experimetal details

Synthesis of enamine-BODIPYs

General: All starting materials and reagents were commercial, unless otherwise indicated, and used without further purifications. Common solvents were dried and distilled by standard procedures. Flash chromatography was performed using silica gel (230-400 mesh). NMR spectra were recorded using $CDCl_3$ at 20 ºC. ^1H NMR and ^{13}C NMR chemical shifts (δ) were referenced to internal solvent $CDCl_3$ (δ = 7.260 and 77.16 ppm, respectively). DEPT 135 experiments were used to determine the type of carbon nucleus (C vs. CH vs. CH_2 vs. CH_3). FTIR spectra were obtained from neat samples using the ATR technique. High resolution mass spectrometry (HRMS) were performed using the EI technique.

Synthesis: BODIPYs **2a-d** (Figure 2 in manuscript) were synthesized by the corresponding described methods.[1]

*Synthesis of **1**:* To a solution of commercially available BODIPY 505/515 (30 mg, 0.12 mmol) in acetic anhydride (2 mL) was added, under argon atmosphere, *N,N*-dimethylformamide dimethyl-acetal (DMF-DMA; 0.08 mL, 0.60 mmol) and the resulting mixture was refluxed for 1 h. After cooling to r.t., hexane was added and stirring maintained for 30 min. Finally, the solvent was removed by vacuum distillation, the residue was washed with hexane and filtered. Compound **1** (31 mg, 83%) was obtained as a purple solid. ^1H NMR (700 MHz, $CDCl_3$) δ 7.20 (d, *J* = 13.3 Hz, 1H, CH), 6.67 (s, 1H, CH), 6.33 (s, 1H, CH), 5.90 (s, 1H, CH), 5.83 (d, *J* = 13.3 Hz, 1H, CH), 3.03 (s, 6H, $2CH_3N$), 2.49 (s, 3H, CH_3), 2.20 (s, 3H, CH_3), 2.19 (s, 3H, CH_3) ppm. ^{13}C NMR (176 MHz, $CDCl_3$) δ 160.4 (C), 149.9 (CH), 146.4 (C), 142.3 (C), 136.4 (C), 131.9 (C), 130.7 (C), 115.4 (CH), 114.9 (CH), 112.0 (CH), 90.1 (CH), 14.3 (CH_3), 11.5 (CH_3), 11.2 (CH_3) ppm (CH_3N not observed). FTIR ν 2921, 2856, 1621, 1596, 1562, 1484, 1416, 1386, 1285, 1246, 1152, 1116, 1064 cm^{-1}. HRMS-EI *m/z* 303.1716 (calcd. para $C_{16}H_{20}BF_2N_3$: 303.1718).

Photophysical characterization

The absorption spectra were recorded by UV-Vis-NIR Spectroscopy (model Cary 7000, Agilent Technologies, Madrid, Spain) equipped with two lamps (halogen lamp for Vis-IR region and deuterium lamp for UV region).

The fluorescence measurements were recorded with an Edinburgh Instruments Spectrofluorimeter (FLSP920 model, Livingston, UK) equipped with a xenon flash lamp 450 W as the excitation source. The fluorescence spectra were corrected from the wavelength dependence on the detector sensibility. The fluorescence quantum yields of the photosensitizers were measured by relative method, using as standard samples: pyrromethene 567 (Φ_{fl} = 0.91 in methanol),[2] pyrromethene 605 (Φ_{fl} = 0.66 in ethanol) and cresyl violet (Φ_{fl} = 0.54 in methanol)[3] for the Visible region.

Radiative decay curves were recorded in the same Edinburgh Instrument by *Time-Correlated Single-Photon Counting Technique* (TC-SPC), using a microchannel plate detector (Hamamatsu C4878) with picoseconds time resolution (≈100 ps). Fluorescence decay curves were monitored at the maximum emission wavelength after excitation using a fianium supercontinuous wavelength tunable-laser with 150 ps FWHM pulses.

Phosphorescence spectra were recorded at 77 K using an Optisa DN cryostat and ITC601 temperature controller (Oxford Instruments) in an ethanol:iodoethanol mixture (9:1).

The singlet oxygen quantum yield (Φ_Δ^{PS}) was determined by direct method measuring its phosphorescence at 1276 nm employing a NIR detector (InGaAs detector, Hamamatsu G8605-23), integrated into the same Edinburgh spectrofluorimeter upon continuous monochromatic excitation (450 W Xenon lamp) of the sample in cells of 1 cm in front configuration (front face), 40° and 50° to the excitation and emission beams, respectively, and leaned 30° to the plane formed by the direction of incidence. The value was obtained by the media of at least five different concentrations (range from $2x10^{-6}$ M to $5x10^{-5}$ M) and using commercial photosensitizers as reference 8-methylthio-2,6-diiodoBODIPY (MeSBDP, CAS-1835282-63-7, Φ_Δ^{PS} = 0.89 in toluene and Φ_Δ^{PS} = 0.91 in $CHCl_3$).[4]

TA spectra in the nanosecond range (ns-TA) and lifetime of triplet state (^{3}PS*) were recorded in Laser Flash Photolysis (LP980, Edinburgh Instruments). Samples were excited with a computer-controller Nd:YAG laser coupled to OPO system from LOTIS (TII 2134) operating at 1 Hz and with a pulse width of 7 ns. The transient spectra were registered in spectral mode with ICCD (Andor's iStar DH320T) and the kinetic decay curves in a PMT detector (Hamamatsu R928). Triplet lifetimes were obtained from the corresponding decay of the triplet transient band at the absorption maximum in the presence (aerated solutions) and absence of oxygen (deaerated solution). Data were analyzed by the LP900 software.

Femtosecond TA (fs-TA) measurements were carried out in solution with solvents with increasing polarity: cyclohexane (c-hexane), toluene, chloroform ($CHCl_3$) and acetonitrile (ACN), at concentrations in the order of $1x10^{-4}$ M. Samples were contained in a 1 mm fused silica cuvette and continuously scanned across the focal plane to avoid thermal effects on the sample. Ultrashort laser pulses were generated in an oscillator-regenerative amplifier laser system (Coherent, Mantis-Legend) that provides a 1 KHz train of 35 fs pulses at 800nm. Pump pulse wavelength around 550 nm is obtained by means of sum frequency of the fundamental 800 nm and the signal beam of an optical parametric amplifier (OPA). The white light continuum probe (320 nm-1 100 nm) is produced by focusing a small fraction of the amplifier output on a 2 mm thick CaF2 window. Pump-probe delay is achieved with a translation stage (Thorlabs, DDS220) that allows a maximum range of 2 ns. Transient absorbance is measured with a fiber-coupled dual channel spectrometer (Avantes, Avaspec) as a function of the pump-probe delay.

The procedure to analyze the fs-TA data is as follows:

First, the spectra were aligned to correct from the broadband pulse chirp by setting zero delay-time reference for each wavelength. Secondly, the spontaneous emission and scattering contributions are removed from the baseline by subtracting a spectrum collected at negative time delays. Then, the probe-wavelength dependent transients were modeled by the convolution function:

$$S(\lambda, t) = \int_{-\infty}^{\infty} M(\lambda, t - t')R(\lambda, t')\, dt'$$

where

$$M(t) = \sum_{i=1}^{4} a_i e^{-t/\tau_i}$$

is a multi-exponential molecular response and R(I,t) the instrumental response function. A global analysis procedure permits to extract a single set of t_i constants for a collection of a_i pre-exponential factors (DAS).

To illustrate the validity of the procedure to extract the rates of the observed processes, Figure S5 (see below) includes the experimental data after chirp and baseline correction for sample *2c* in ACN, together with the results of the analysis and the residuals of the fitting.

Electronic structure calculations

Ground state molecular geometries have been optimized within the density functional theory (DFT) in conjunction with the CAM-B3LYP exchange-correlation functional[5] and the 6-311+G(d) basis set. Electronic transitions and excited state minima have been obtained with the (linear response) time-dependent DFT (TDDFT) using the same energy functional and the cc-pVDZ, which has shown good results in the computation of low-lying excitations of BODIPY.[6] Spin-orbit couplings between singlet and triplet states have been obtained at the CAM-B3LYP/cc-pVDZ computational level by means of the Breit-Pauli Hamiltonian[7] and disregarding two-electron contributions.[8] Solvent effects were taken into account by the polarized continuum model (PCM).[9,10] All calculations have been performed with the Q-Chem program.[11]

In vitro assays

Cells culture

Human cervix adenocarcinoma HeLa cells obtained from ATCC were grown in Dulbecco´s modified Eagle´s medium (DMEM) supplemented with 10% (v/v) fetal bovine serum (FSB) and 50 U/mL penicillin and 50 mg/mL streptomycin, in a humidified 5% CO_2 cells incubator at 37 ºC. For the cell viability assays, cells were grown to monolayer.

Sample preparation

Initial solutions of **1** and **2d** ($2.5x10^{-3}$ M) were prepared in DMSO (Dimethyl sulfoxide, Pancreac, Barcelona, Spain) and diluted in culture medium to the desired concentration prior to incubation with cells. Final amount of DMSO in culture medium did not exceed the 1% in any experimental conditions due to its associate toxic effects for cells.

Subcellular localization

For internalization and subcellular localization studies, cells were seeded in coverslips in glass-bottom 35 mm petri dishes and subconfluent monolayers were used. Localization of compounds **1** and **2d** (10 μM for 24 h) in living HeLa cells was studied by optical microscopy (Phase contrast and fluorescence). Images were obtained with an Olympus BX61 epifluorescence microscope equipped with an Olympus DP50 digital camera (Olympus, Center Valley, PA, USA), and processed with Photoshop CS5 software (Adobe Systems). The following excitation filters were used in order to visualize the fluorescence signal of compounds: UV (360-390 nm), blue (460-490 nm) and green (510-550 nm).

Subcellular accumulation pattern of **1** and **2d** were compared with that of the following organelle-targeted fluorescent probes: dipid droplets by BODIPY 493/503 (40 µM, 10 min; ThermoFisher, Waltham, MA, USA) and OIL RED O (Staining Kit K580-24, BioVision, San Francisco, CA, USA). Staining was performed following the kit instructions), mitochondria with MitoTracker Green/ MitoTracker Red (75 nM, 30 min; ThermoFisher) or LysoTracker Green/LysoTracker Red (50 nM, 30 min; ThermoFisher) in the culture medium at 37 °C in the same conditions. After labeling, coverslips were washed with PBS and observed immediately by fluorescence microscopy.

Different excitation filters were used for fluorescent probes analyzed. BODIPY 493/503 was observed under blue excitation filter, OIL RED O under green filter; MitoTracker Green and MitoTracker Red under blue and green light, respectively; and LysoTracker Green and LysoTracker Red under blue and green excitation filter, respectively.

Photodynamic treatments

For photodynamic therapy studies, cells were seeded in 24 well plates. Subconfluent monolayers of cells were incubated for 24 h with 1, 2.5, 5, 7.5 and 10 µM of **2d** in 10% FBS cell culture medium. After 24 h exposure, cells were washed three times with culture medium without FBS and maintained in the culture medium during irradiation and post-treatment time (24 h). Irradiations were performed with green light (518 ± 10 nm) using a light-emitting diode (LED) device (LED Par 64 Short Q4-18, Showtec, Burgebrach, Holland), using a total light dosage of 10 Jcm^{-2}. Parallel experiments were carried out by incubating the cells with **2d** without irradiation to test their dark toxicity. MTT assay was used to determine cell viability after each treatment. 24 h after treatments, cells were incubated with 50 µg/mL solution of 3-(4,5-dimethylthiazol-2-yl)-2,5-diphenyltetrazolium bromide (MTT; Sigma Aldrich, Saint Louis, MO, USA) in culture medium for 3 h. Then, culture medium was removed, reduced formazan was diluted in DMSO and optical absorbance was measured at 542 nm in a SpectraFluor spectrophotometer (Tecan Group Ltd, Männedorf, Switzerland). Statistical significance for surviving-fraction data acquired from the conducted MTT assays was obtained by using one-way ANOVA. At least 6 replicates of each treatment were used, and experiments were repeated three times.

2. ^{1}H NMR (700 MHz, $CDCl_3$) and ^{13}C NMR (176 MHz, $CDCl_3$) spectra of 1

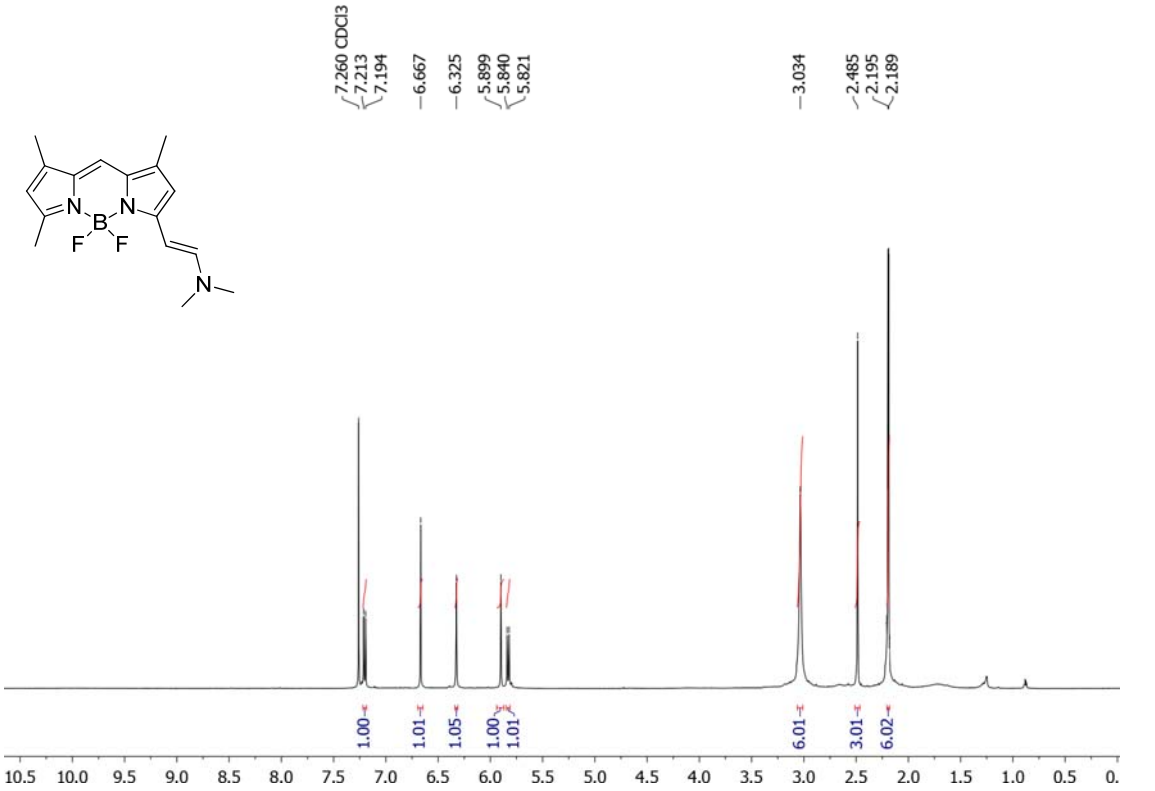

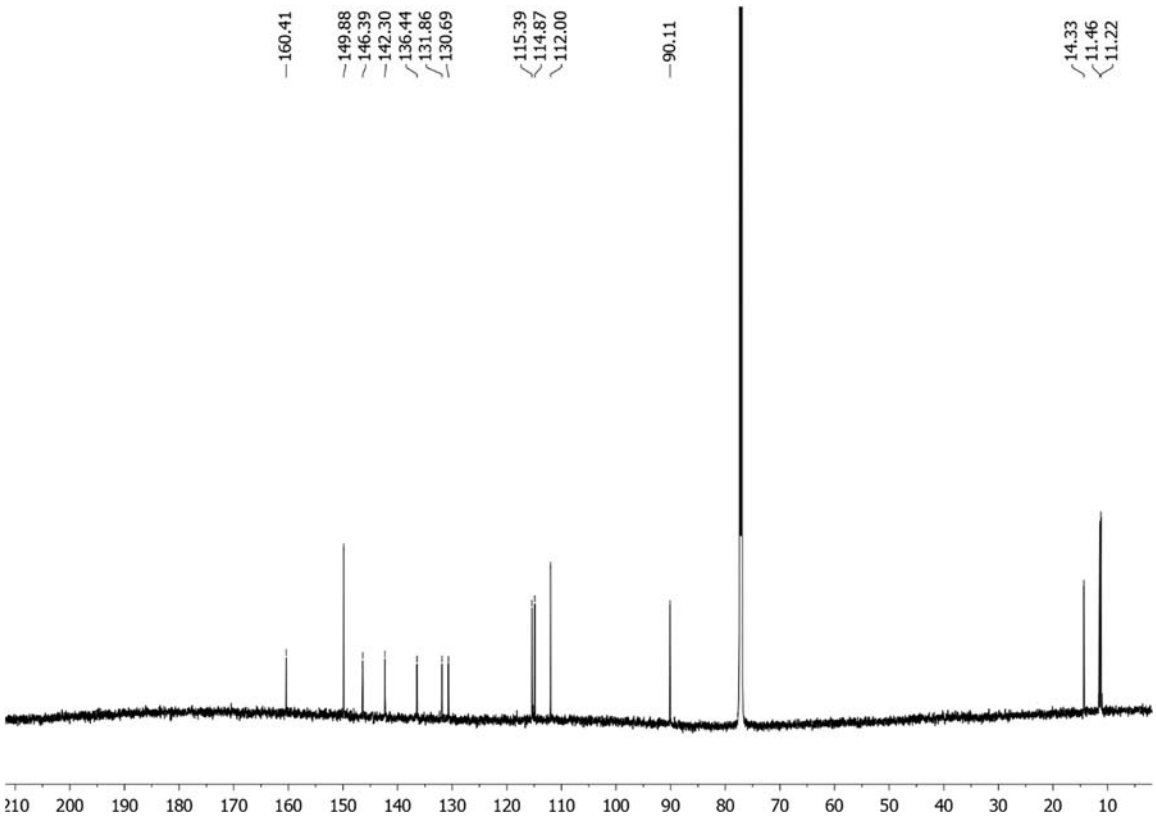

3. Electronic Structure Calculations

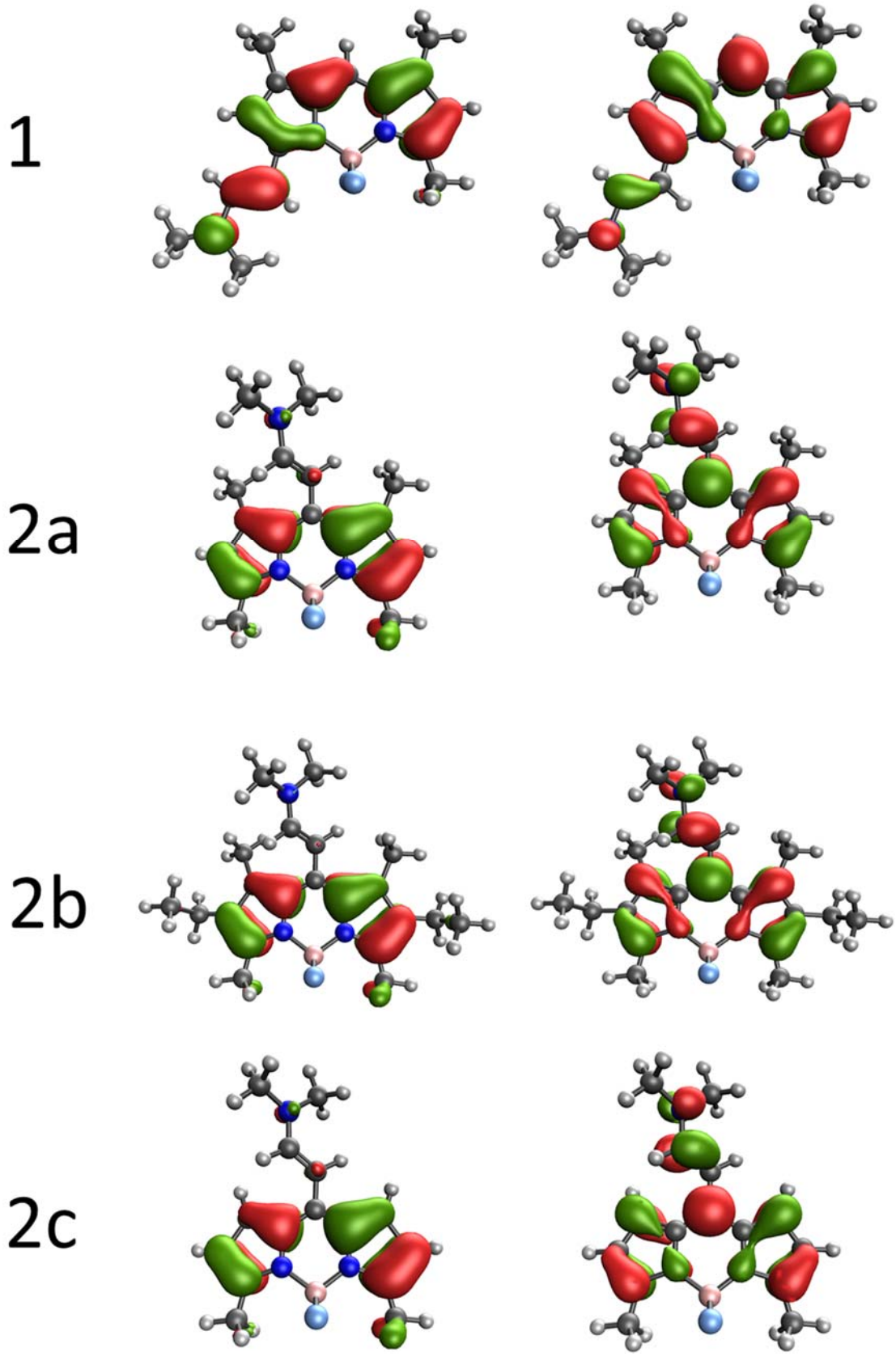

Figure S1. HOMO (left) and LUMO (right) of **1, 2a, 2b** and **2c** computed at the CAM-B3LYP/cc-pVDZ level in chloroform.

Table S1. Vertical excitation energy (eV) and osc. strength of **1** and **2a** computed at the CAM-B3LYP/cc-pVDZ level in chloroform.

Structure	E_{S1}	Strength
1	2.57	1.0657
2a	2.17	$3.5 \cdot 10^{-3}$

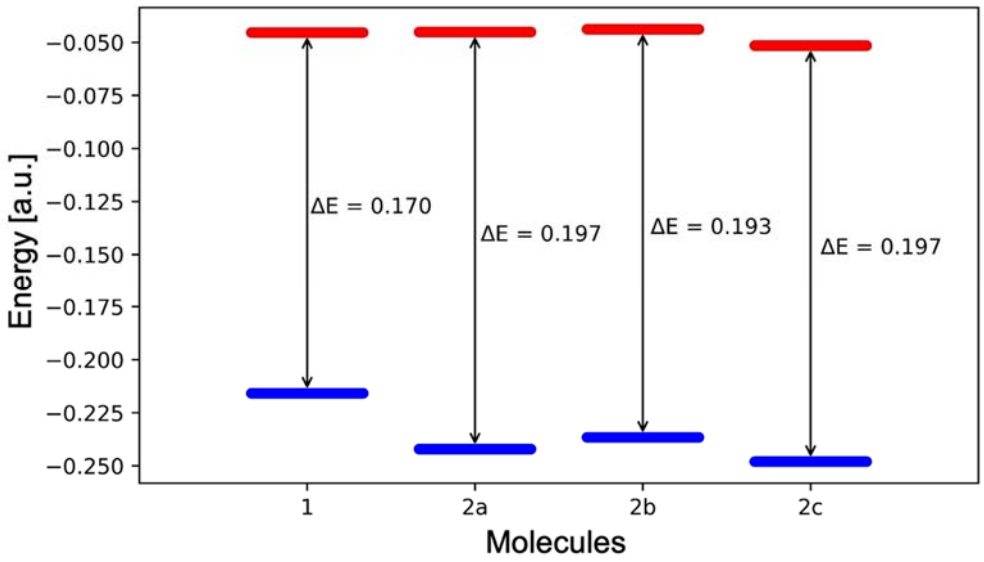

Figure S2. HOMO /LUMO energy diagram of **1**, **2a**, **2b** and **2c** structures in computed at the CAM-B3LYP/cc-pVDZ level in chloroform.

Table S2. S_0/S_1 vertical energies (eV) and osc. strength (in parenthesis) at 20 and 90 dihedral angles for **2c** in cyclohexane and acetonitrile and their relative change (ΔE).

Character	Cyclohexane	Acetonitrile	ΔE
Local Excitation	2.83 (0.6330)	2.86 (0.6761)	0.03
Charge Transference	2.12 ($1.4 \cdot 10^{-3}$)	1.85 ($6.0 \cdot 10^{-4}$)	0.27

4. Photophysical properties

Table S3. Photophysical properties and singlet oxygen quantum yield in different solvents for **2a**, **2c, 2b** and **2d**; absorption maxima (λ_{ab}), molar absorption coefficient (ε_{max}), fluorescence maxima (λ_{fl}), fluorescence quantum yield (Φ_{fl}), fluorescence lifetime (τ_{fl}) and singlet oxygen quantum yield (Φ_{Δ}).

Sample	Solvent	λ_{ab} (nm)	λ_{fl} (nm)	Φ_{fl}	τ_{fl} (ns)	Φ_{Δ}
2a	Toluene	498.0	520.0	0.01	0.60(48%) 5.13(52%)	0.12
	$CHCl_3$	494.0	517.0	0.01		0.04
	ACN[1]	475.0	505.5	<0.01	-	-
2b	Toluene	519.0 447.0	541.5	0.04	5.16	0
	$CHCl_3$	516.0 449.0	543.0	<0.01	-	0
	ACN[1]	499.0 (459.0)	536.0	<0.01	-	-
2c	Toluene	498.0	535.5	0.22	1.83(87%) 2.94(13%)	0.37
	$CHCl_3$	496.0	529.0	0.04	0.92(97%) 5.29 (3%)	0.20
	ACN[1]	487.0	506.0	<0.01	-	-
2d	Toluene	551.0	601.0	0.46	3.29	0.38
	$CHCl_3$	551.0	599.0	0.42	3.23	0.31
	ACN[1]	533.0	551.0	0.04	0.43	-

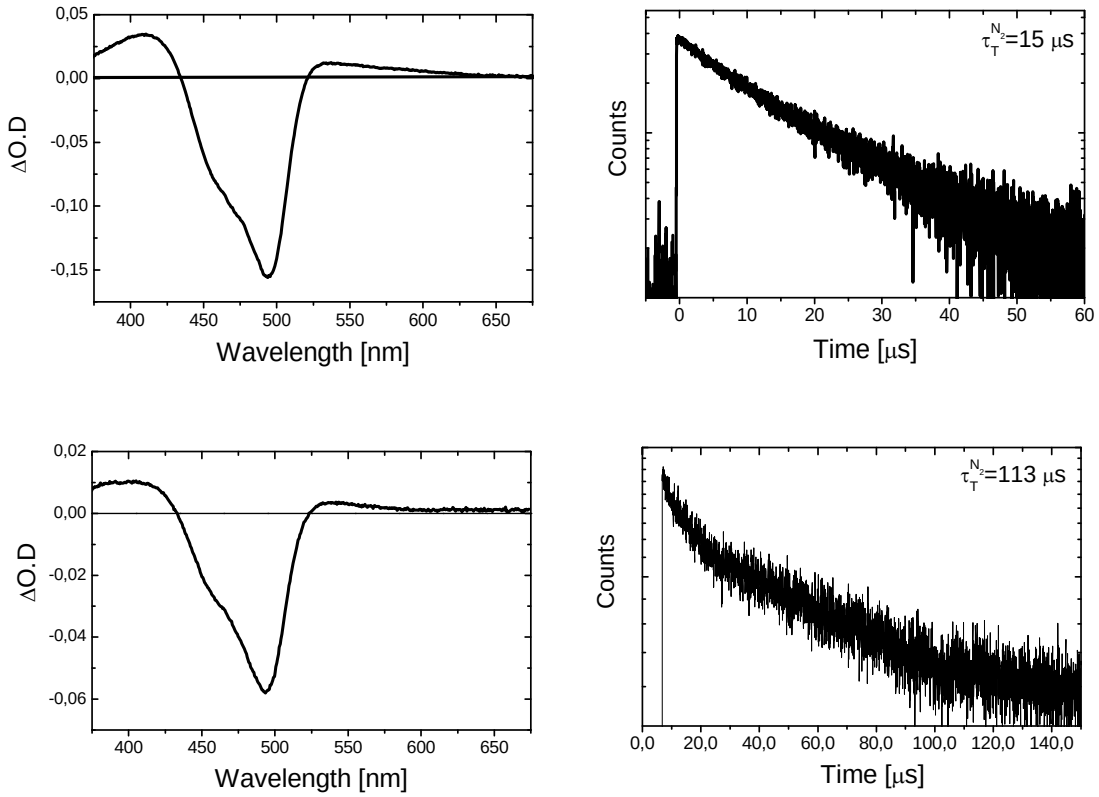

Figure S3. ns-TAS (left) and decay curve of transient triplet band of **2c** (right) in deaerated toluene (top) and chloroform (bottom).

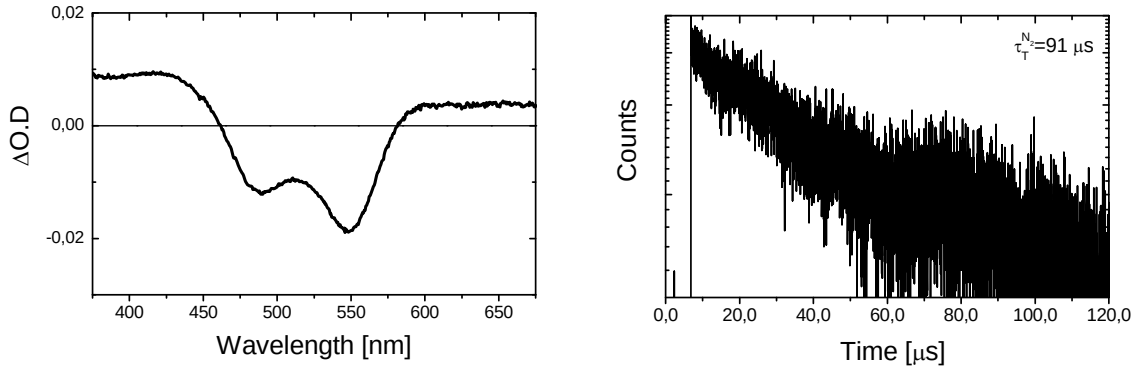

Figure S4. ns-TAS (left) and decay curve of transient triplet band of **2d** (right) in deaerated chloroform. Similarly as ns-TAS of **2c**, he recorded spectra for **2d** present a positive band at around 375-450 nm which is attributed to the absorption of the T1 state. The negative contribution in the 450-595 nm correspond to the ground state bleaching (GSB) associated with the S0→S1 transition. Finally, the weak and broad contribution at >595 nm for **2d** is also attributed to triplet absorption. After tail fiting of the decay curve registered at 420 nm, the triplet lifetime value obtained is 91 μs.

Table S4. Triplet lifetime in nitrogen- and air-saturated samples (τ^T_0 and τ^T_{air}, respectively) of **2c** and **2d**

		τ^T_0 (μs)	τ^T_{air} (μs)
2c	**toluene**	16	0.375
	chloroform	113	0.428
2d	**chloroform**	91	0.420

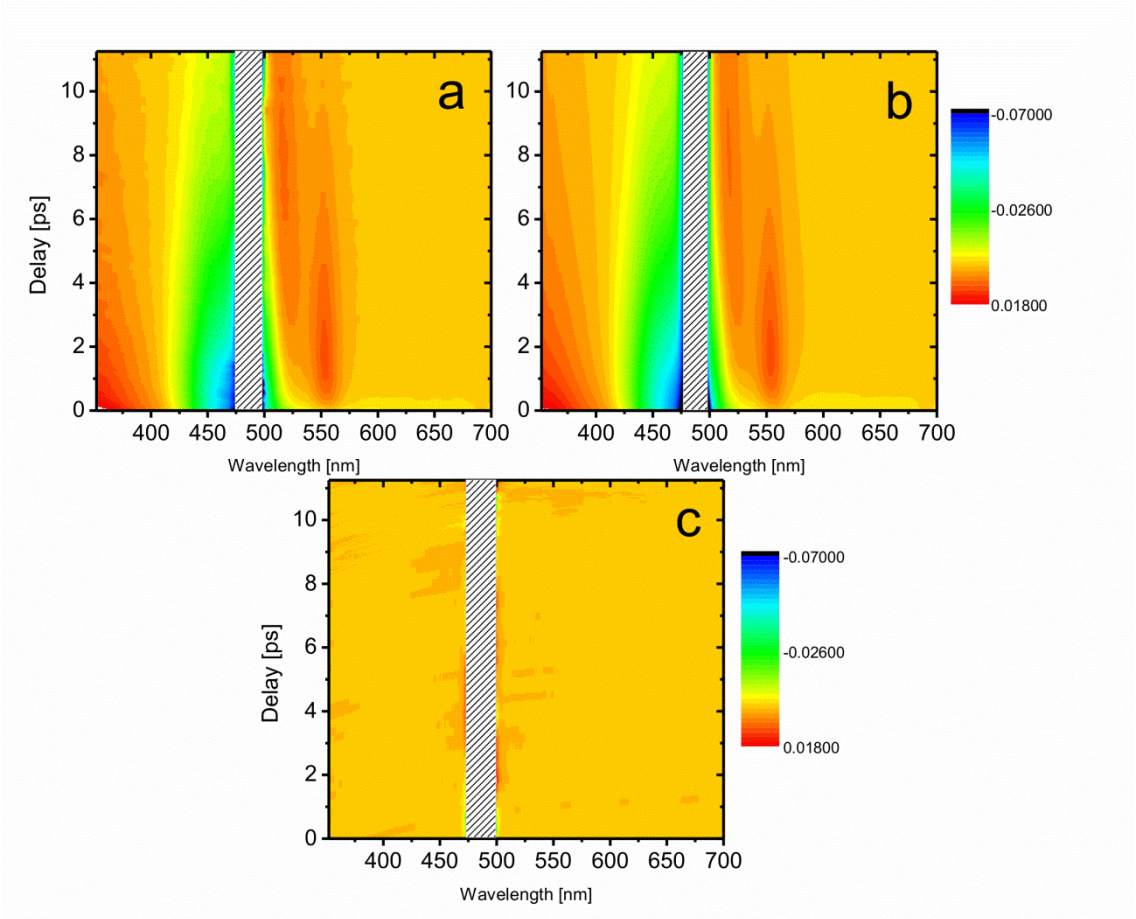

Figure S5. a) TA data recorded for sample 2c in ACN. b) Results of the fitting procedure. c) Residuals of the fitting.

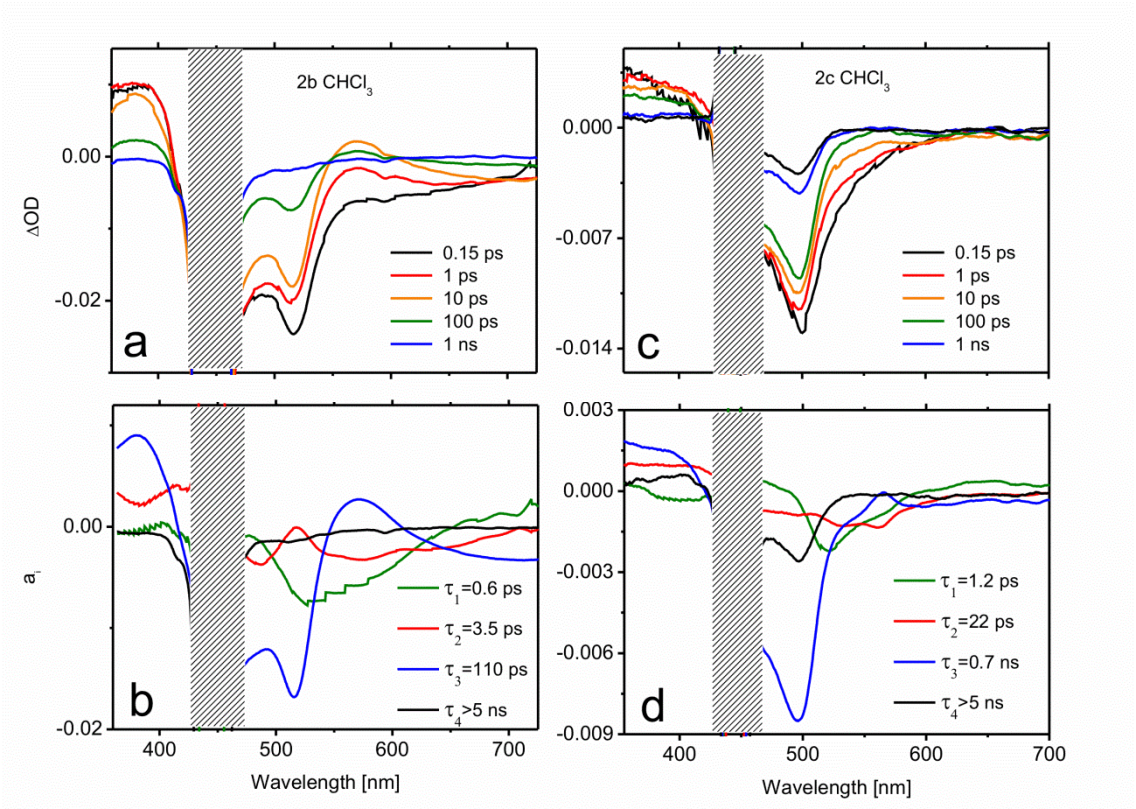

Figure S6. Transient spectra and DAS of **2b** (a, b) and **2c** (c, d) in $CHCl_3$.

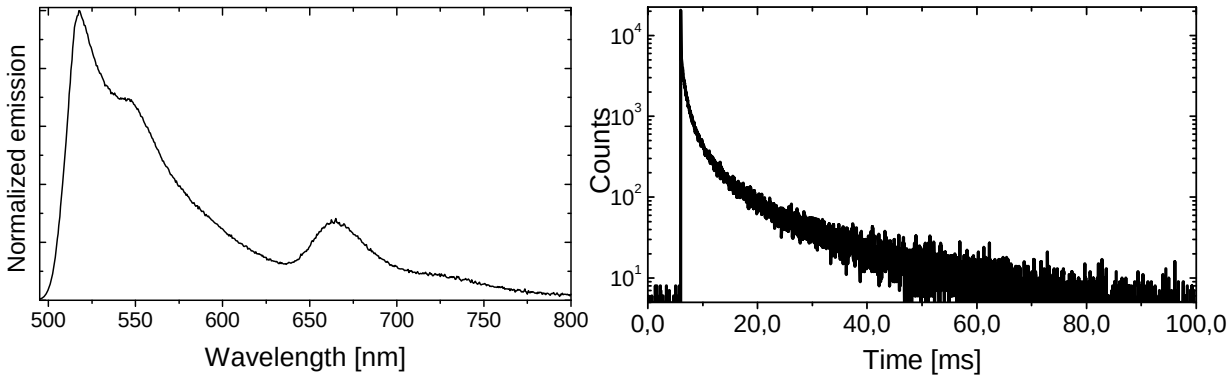

Figure S7. A) Luminescence spectra at 78 K of compound **2c** in EtOH solution with a 10% of iodoethane B) decay curve registered at the maximum of the phosphorescence band. The phosphorescence decay curve was analyzed as bi-exponential and two phosphorescence lifetimes were obtained, τ_{ph}: 5.4 ms (75%) and 25 ms (25%).

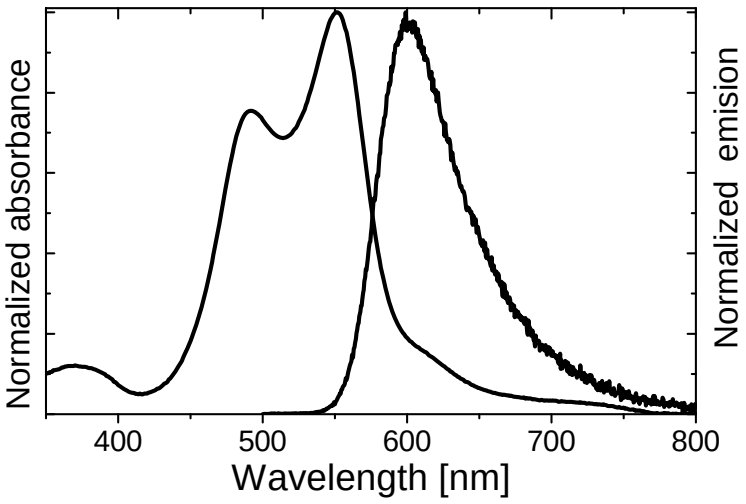

Figure S8. Height-normalized absorption and emission spectra for **2d** in chloroform

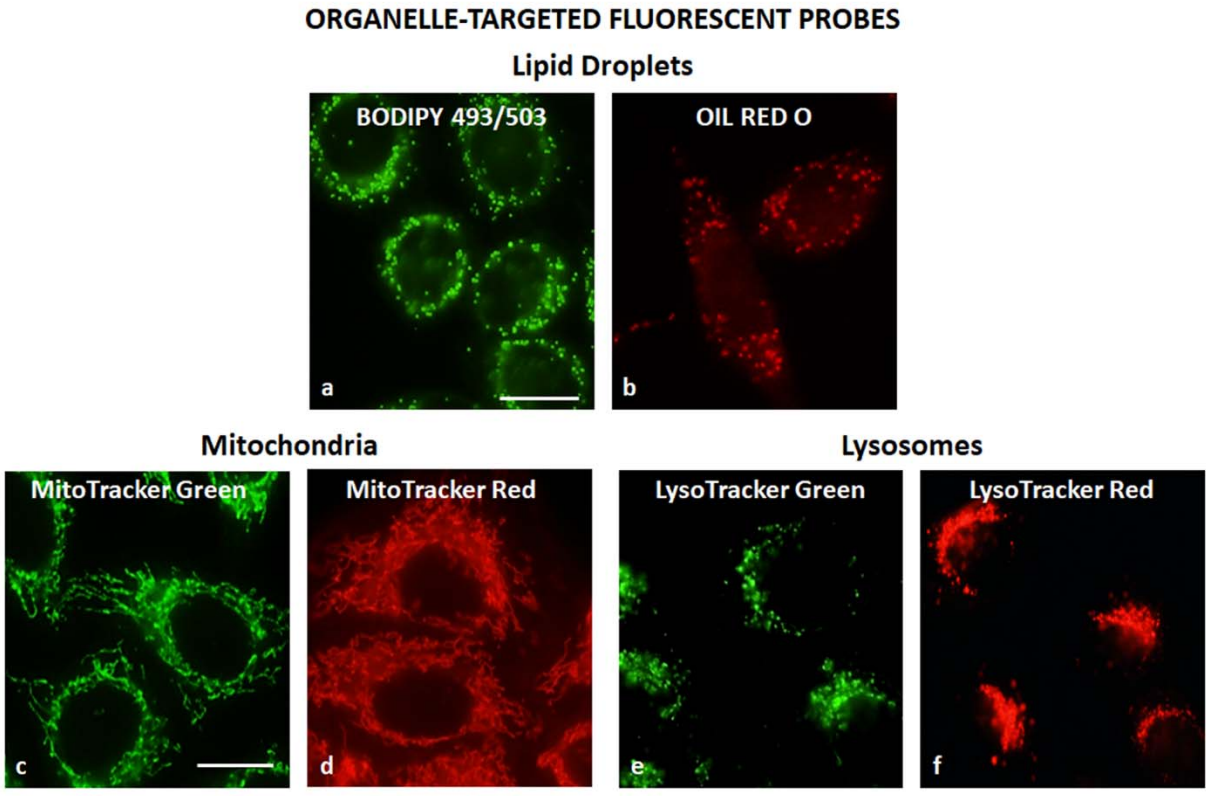

Figure S9. Representative images of intracellular distribution of lipid droplets, mitochondria and lysosomes in HeLa cells using different fluorescent probes. Lipid Droplets-Targeted Probes: BODIPY 493/503 (a) and Oil Red O (b); Mitochondrion-Targeted Probes: MitoTracker Green (c) and MitoTracker Red (d); Lysosome-Targeted Probes: LysoTracker Green (e) and LysoTracker Red (f). Scale bar: 10 μm.

5. References

(1) Palao-Utiel, E.; Montalvillo-Jiménez, L.; Esnal, I.; Prieto-Montero, R.; Agarrabeitia, A. R.; García-Moreno, I.; Bañuelos, J.; López-Arbeloa, I.; de la Moya, S.; Ortiz, M. J. Controlling Vilsmeier-Haack Processes in Meso-MethylBODIPYs: A New Way to Modulate Finely Photophysical Properties in Boron Dipyrromethenes. *Dyes and Pigments* **2017**, *141*, 286–298. https://doi.org/10.1016/j.dyepig.2017.02.030.

(2) López Arbeloa, F.; López Arbeloa, T.; López Arbeloa, I.; García-Moreno, I.; Costela, A.; Sastre, R.; Amat-Guerri, F. Photophysical and Lasing Properties of Pyrromethene 567 Dye in Liquid Solution.: Environment Effects. *Chemical Physics* **1998**, *236* (1–3), 331–341. https://doi.org/10.1016/S0301-0104(98)00215-8.

(3) Magde, D.; Brannon, J. H.; Cremers, T. L.; Olmsted, J. Absolute Luminescence Yield of Cresyl Violet. A Standard for the Red. *Journal of Physical Chemistry* **1979**, *83* (6), 696–699. https://doi.org/10.1021/j100469a012.

(4) Prieto-Montero, R.; Sola-Llano, R.; Montero, R.; Longarte, A.; Arbeloa, T.; López-Arbeloa, I.; Martínez-Martínez, V.; Lacombe, S. Methylthio BODIPY as a Standard Triplet Photosensitizer for Singlet Oxygen Production: A Photophysical Study. *Physical Chemistry Chemical Physics* **2019**, *21* (36), 20403–20414. https://doi.org/10.1039/C9CP03454D.

(5) Yanai, T.; Tew, D. P.; Handy, N. C. A New Hybrid Exchange – Correlation Functional Using The. **2008**, *393* (2004), 51–57. https://doi.org/10.1016/j.cplett.2004.06.011.

(6) Postils, V.; Ruipérez, F.; Casanova, D. Mild Open-Shell Character of BODIPY and Its Impact on Singlet and Triplet Excitation Energies. *Journal of Chemical Theory and Computation* **2021**, *17* (9), 5825–5838. https://doi.org/10.1021/acs.jctc.1c00544.

(7) Bethe, H. A.; Salpeter, E. E. *Quantum Mechanics of One- and Two-Electron Atoms*; Springer US, 1977. https://doi.org/10.1007/978-1-4613-4104-8.

(8) Ou, Q.; Subotnik, J. E. Electronic Relaxation in Benzaldehyde Evaluated via TD-DFT and Localized Diabatization: Intersystem Crossings, Conical Intersections, and Phosphorescence. *Journal of Physical Chemistry C* **2013**, *117* (39), 19839–19849. https://doi.org/10.1021/jp405574q.

(9) Cancès, E.; Mennucci, B. Comment on "Reaction Field Treatment of Charge Penetration" [J. Chem. Phys. 112, 5558 (2000)]. *Journal of Chemical Physics* **2001**, *114* (10), 4744–4745. https://doi.org/10.1063/1.1349091.

(10) Chipman, D. M. Energy Correction to Simulation of Volume Polarization in Reaction Field Theory. *Journal of Chemical Physics* **2002**, *116* (23), 10129–10138. https://doi.org/10.1063/1.1477928.

(11) Epifanovsky, E.; Gilbert, A. T. B.; Feng, X.; Lee, J.; Mao, Y.; Mardirossian, N.; Pokhilko, P.; White, A. F.; Coons, M. P.; Dempwolff, A. L.; et al. Software for the Frontiers of Quantum Chemistry: An Overview of Developments in the Q-Chem 5 Package. *The Journal of chemical physics* **2021**, *155* (8), 084801–084859. https://doi.org/10.1063/5.0055522.